

Registration of H₂O and SiO masers in the Calabash Nebula, to confirm the Planetary Nebula paradigm

R., Dodson¹, M. Rioja^{1,2,3}, V. Bujarrabal³, J. Kim⁴, S. H. Cho⁵,
Y. K. Choi⁵ and Y. Youngjoo⁵

¹International Centre for Radio Astronomy Research, UWA, 35 Stirling Hwy, Western Australia

²CSIRO Astronomy and Space Science, 26 Dick Perry Avenue, Kensington WA 6151, Australia

³Observatorio Astronómico Nacional (IGN), Alfonso XII, 3 y 5, 28014 Madrid, Spain

⁴Shanghai Astronomical Observatory, Chinese Academy of Sciences, Shanghai 200030, China

⁵Korea Astronomy and Space Science Institute 776, Daedeokdae-ro, Yuseong-gu, Daejeon, 34055, Republic of Korea

Abstract. We report on the astrometric registration of VLBI images of the SiO and H₂O masers in OH 231.8+4.2, the iconic Proto-Planetary Nebula also known as the Calabash nebula, using the KVN and Source/Frequency Phase Referencing. This, for the first time, robustly confirms the alignment of the SiO masers, close to the AGB star, which drives the bi-lobe structure with the water masers in the out-flow.

Keywords. stars: individual: QX Pup – stars: AGB and post-AGB – masers – stars: evolution

1. Introduction

OH 231.8+4.2 (OH 231) is perhaps the best studied proto-Planetary Nebulae (pPN), and in many ways provides the prototype for the class. pPN develop from Asymptotic Giant Branch (AGB) stars, into the environment seeded by the previous copious AGB mass-loss, which forms a thick spherical circumstellar envelope (CSEs). These pPN occur when the AGB completes throwing off the outer stellar layers, when the stellar core becomes exposed becoming the new central star. This new star is very compact, rapidly evolving to the blue and white dwarf phase. In at least some cases there are also fast moving jets carrying significant angular momentum. At present, the only way to explain the origin of such energetic flows is to assume that a fraction of the ejected CSE is re-accreted by the central star or a companion through a rapidly rotating disk. The CSE is shocked by very fast bipolar outflows from the dwarf, with axial velocities as high as several hundred km s⁻¹. These generate a series of axial shocks that cross the massive CSE, inducing high axial velocities in it. The blue dwarf at the centre is able to significantly ionize the nebula, revealing its wide bipolar shape and producing some of the most beautiful objects in the sky.

SiO masers are known to form close to AGB stars, and water masers form in outflows so together they probe the crucial jet/shock regions. However as soon as the star+nebula system leaves the AGB phase the observation of the masers associated with them becomes more and more difficult. The reason is that the inner circumstellar masers are becoming more and more diffuse at the same time as the mass-loss rate decreases, therefore SiO masers are very rarely observed. However there is one, paradigmatic, example showing both SiO and H₂O masers: the strongly bipolar nebula OH 231, the Calabash Nebula, which shows the classic bi-polar structure. OH 231 has a binary central source, which has

been identified through optical spectroscopy; a M9-10 III Mira variable (i.e. an AGB star) (Cohen 1981) and a A0 main sequence companion (Sánchez Contreras *et al.* 2004). This remarkable bipolar nebula shows all the signs of post-AGB evolution: fast bipolar outflows with velocities $\sim 200 - 400 \text{ km s}^{-1}$, shock-excited gas and shock-induced chemistry.

VLBI observations of SiO and H₂O masers with the VLBA have yielded a number of important results (for example, see Sánchez Contreras *et al.* 2002; Desmurs *et al.* 2007; Choi *et al.* 2012; Leal-Ferreira *et al.* 2012). Water vapour emission comes from two regions in opposite directions along the nebula axis and presumably the H₂O clumps represent the inner nebula, at the base of the bipolar flow. SiO masers occupy smaller regions and lie almost exactly perpendicular to the axis. The movements depicted by the observations of SiO are compatible with a disk orbiting the central star(s) (Sánchez Contreras *et al.* 2002). In principle, we are seeing in this object the whole central structure of disk plus outflow that would confirm our ideas on the post-AGB nebular dynamics. However the astrometric information in these observations is either missing or poor; the SiO observations of Sánchez Contreras *et al.* (2002) and H₂O observations of Leal-Ferreira *et al.* (2012) were self-calibrated, so have no absolute positions. The joint observations of H₂O and SiO by Desmurs *et al.* (2007) are phase referenced, but the SiO $v=2$ detection is only ‘tentative’, and no image nor spectrum is provided.

The SiO transition, because of its high excitation energy, is believed to always mark the location of the central AGB-star (Elitzur 1992). Therefore, whilst it is logical that the SiO/AGB-star is at the center of nebulae, between the H₂O clusters, definitive astrometry is required to allow solid conclusions on the disk/outflow association. Efforts over the last decade to provide the registration have been unsuccessful. The main reason for this is that conventional phase referencing at mm-wavelengths is extremely challenging and that the masers weaken as they expand away from the central star. In this paper we present bona-fide astrometric registration of the SiO emission to the positions of the H₂O masers using Source Frequency Phase Referencing (SFPR), with the H₂O registered to an absolute frame using conventional phase referencing.

2. Observational Details

OH 231 was observed by the Korean VLBI Network (KVN) on 25 Jan, 2017 (N17RD01A) with simultaneous 12mm and 7mm frequencies, each recording 4, dual polarisation, Intermediate Frequency (IF) bands of 16-MHz width. These were spread to cover the H₂O and $v=2,1 \text{ J} \rightarrow 0$ transitions at 22235.044, 42820.57 and 43122.09-MHz respectively and provide the maximum frequency span compatible with the backend (64-MHz at 22-GHz and 382-MHz at 43-GHz), to provide accurate delay measurements.

The KVN has a truly unique capability: simultaneous frequency phase referencing between bands, which registers the high frequency, mm-wave image against the low frequency image, allowing the measurement of the change of source structure across the frequency bands. Examples demonstrated include core-shifts for AGNs (Rioja *et al.* 2014, 2015, 2017) and spatial relationships between maser transitions (Dodson *et al.* 2014; Yoon *et al.* 2017, for H₂O and SiO). We used the latter to derive the relative astrometric separation of the H₂O and SiO masers in OH 231.

3. Results and Discussion

We measured the residual delays from J0746-1555 at 22GHz, and the phases from a point source model-fit to the strongest channel of the H₂O maser. These were applied to the whole H₂O maser dataset. These results were also scaled up and applied to the

SiO maser datasets, following the method presented in Dodson *et al.* (2014), placing the H₂O and SiO masers on a common reference frame. Figure 1 shows the relative phase referenced positions of the detected emission at epoch 2017.07 in J2000. The absolute positions of the strongest features are in Table 1.

Absolute position errors are those for the calibrator, which is 0.3mas. The relative position error for referencing between 22/43-GHz would be dominated by the absolute position error of the H₂O maser position and the fractional bandwidth $\Delta\nu/\nu$, that is 0.15 mas. However the dominant relative position error between SiO features will be that from the beam size over the SNR for the individual spots. For the strongest feature this is ~ 0.2 mas, but for the median spot flux this is ~ 0.5 mas.

Maser Transition	Velocity (km s ⁻¹)	RA 07:42:s	Dec -14:42:s	Error (μ as)
H ₂ O	27.5–29.5	16.91525	50.02167	40
SiO v=1	35–38	16.915379	50.06995	10
SiO v=2	33–38	16.915371	50.06963	10

Table 1: Absolute positions for strongest integrated maser feature as observed on 2017/01/25, with the velocity range of the feature and fitting errors.

We find, as expected and suggested tentatively in Desmurs *et al.* (2007), that the SiO masers are placed in the center of the H₂O distribution, but slightly shifted to the North with respect to the H₂O centroid. This result is compatible with the general trend of this nebula to show more extended southern lobes, notably in the wide optical and CO images. The SiO+H₂O images (Fig. 1) is amazingly similar to a reduced version of the optical image, scaled down by a factor ~ 500 . Our data also confirm the general structure of the SiO-emitting region, Fig. 2: elongated and perpendicular to the nebular axis found at larger scales. We can so confirm the detection of an equatorial torus-like structure placed in the very center of this strongly bipolar nebula. If, as usually assumed, the SiO spots are placed in a region tightly surrounding the late-type star, that star is shown to be accurately placed in the center of the nebula.

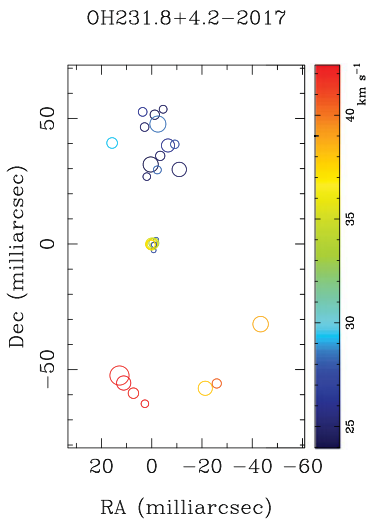


Figure 1. Phase Referenced spot map of H₂O, SiO $v=1$ and $v=2$ $J=1 \rightarrow 0$ masers in OH 231. The SiO emission is at the centre with the H₂O emission in clusters to the North and South. See Dodson *et al.* (2017) for details.

We are able to detect emission at ~ 28 and ~ 36 km s⁻¹ for both the $J=1 \rightarrow 0$, $v=1$ and 2 masers. The lines themselves are very broad (~ 0.4 km s⁻¹), and may well be blended because of the KVN resolution, which is 4×3 mas at 43 GHz. However, we did not detect the emission at 40–43 km s⁻¹ found by Sánchez Contreras *et al.* (2002) and other authors. The KVN resolution, even at 43 GHz, does not allow a detailed investigation of the structure of the SiO-emitting region. Moreover, the whole emission in our data just occupies about 3 mas (Fig. 2), much smaller than the total region detected by Sánchez Contreras *et al.* (2002),

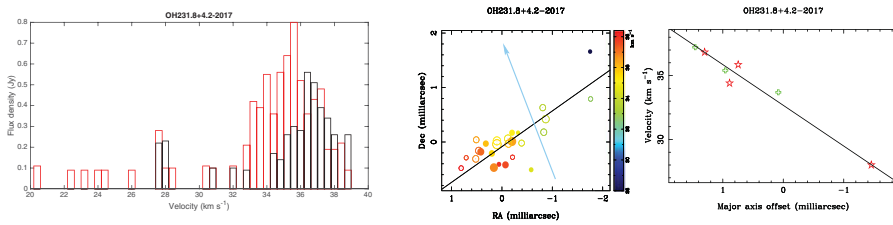


Figure 2. *a)* The spectrum of the detected spots (formed from the clean components) in SiO $v=1$ (blue) and $v=2$ (red) masers, clipped at $0.05 J_y$, showing that both transitions have emission around 28 and 36 km s^{-1} . *b)* The positions of both $v=1,2$ SiO masers coloured to match the velocity scale on the side bar. All the detected channels that contribute to the spot features are plotted separately, with $v=1$ in open circles and $v=2$ in filled circles. The circle size is proportional to the flux. The light blue line marks the expected axis of symmetry, based on the large scale structure. *c)* the velocity-position plots of the SiO maser emission at $J=1 \rightarrow 0$, $v=1$ (green cross) and 2 (red star). The enclosed mass, assuming that all emission is detected, would be $0.05 M_{\odot}$.

~ 8 mas. It is obvious that only a fraction of the torus found by those authors is detected in our data. We only can conclude that our observations are not incompatible with their model torus.

These issues, and measurements of the temporal development of this iconic pPN will be addressed with future deeper, higher resolution, observations with the VLBA, also using SFPR.

References

- Choi, Y. K., Brunthaler, A., Menten, K. M., & Reid, M. J. 2012 (July). Pages 407–410 of: Booth, R. S., Vlemmings, W. H. T., & Humphreys, E. M. L. (eds), *Cosmic Masers - from OH to H0*. IAU Symposium, vol. 287.
- Cohen, M. 1981. *PASP*, **93**(June), 288–290.
- Desmurs, J.-F., Alcolea, J., Bujarrabal, V., Sánchez Contreras, C., & Colomer, F. 2007. *A&A*, **468**(June), 189–192.
- Dodson, R., *et al.*, 2014. *AJ*, **148**(Nov.), 97.
- Dodson, R., Rioja, M. J., Bujarrabal, V., Kim, J., Cho, S. H., Choi, Y. K. & Youngjoo, Y., 2017. *MNRAS*, *Submitted*
- Elitzur, M. (ed). 1992. *Astronomical masers*. Astrophysics and Space Science Library, vol. 170.
- Leal-Ferreira, M. L., Vlemmings, W. H. T., Diamond, P. J., Kemball, A., Amiri, N., & Desmurs, J.-F. 2012. *A&A*, **540**(Apr.), A42.
- Rioja, M., Dodson, R., Gómez, J., Molina, S., Jung, T., & Sohn, B. 2017. *Galaxies*, **5**(Jan.), 9.
- Rioja, M. J., 2014. *AJ*, **148**(Nov.), 84.
- Rioja, M. J., Dodson, R., Jung, T., & Sohn, B. W. 2015. *AJ*, **150**(Dec.), 202.
- Sánchez Contreras, C., Desmurs, J. F., Bujarrabal, V., Alcolea, J., & Colomer, F. 2002. Submilliarcsecond-resolution mapping of the 43 GHz SiO maser emission in the bipolar post-AGB nebula OH231.8+4.2. *A&A*, **385**(Apr.), L1–L4.
- Sánchez Contreras, C., Gil de Paz, A., & Sahai, R. 2004. *ApJ*, **616**(Nov.), 519–524.
- Yoon, D. H., Cho, S. H., Yun, Y. J., Choi, Y. H., Dodson, R., Rioja, M., Kim, J., Kim, D., Yang, H., H., Imai, & Byun, D. Y. 2017. *Nature*, *Submitted*.